

DTIC FILE COPY (2)

NAVAL POSTGRADUATE SCHOOL Monterey, California

AD-A195 586



THESIS

DTIC
ELECTE
JUN 03 1988
S H D

AUTOMATIC DATA RETRIEVAL
FROM ROCKET MOTOR HOLOGRAMS

by

Emin Sami Orguc

December 1987

Thesis Advisor

John P. Powers

Approved for public release; distribution is unlimited.

88 0 1 107

REPORT DOCUMENTATION PAGE

1a. REPORT SECURITY CLASSIFICATION UNCLASSIFIED			1b. RESTRICTIVE MARKINGS			
2a. SECURITY CLASSIFICATION AUTHORITY			3. DISTRIBUTION / AVAILABILITY OF REPORT Approved for public release; distribution is unlimited.			
2b. DECLASSIFICATION / DOWNGRADING SCHEDULE			4. PERFORMING ORGANIZATION REPORT NUMBER(S)			
4. PERFORMING ORGANIZATION REPORT NUMBER(S)			5. MONITORING ORGANIZATION REPORT NUMBER(S)			
6a. NAME OF PERFORMING ORGANIZATION Naval Postgraduate School		6b. OFFICE SYMBOL (If applicable) 32		7a. NAME OF MONITORING ORGANIZATION Naval Postgraduate School		
6c. ADDRESS (City, State, and ZIP Code) Monterey, California 93943-5000			7b. ADDRESS (City, State, and ZIP Code) Monterey, California 93943-5000			
8a. NAME OF FUNDING / SPONSORING ORGANIZATION Air Force Rocket Propulsion Lab		8b. OFFICE SYMBOL (If applicable)		9. PROCUREMENT INSTRUMENT IDENTIFICATION NUMBER		
8c. ADDRESS (City, State, and ZIP Code) Edwards Air Force Base, California, 93523			10. SOURCE OF FUNDING NUMBERS			
			PROGRAM ELEMENT NO.	PROJECT NO.	TASK NO.	WORK UNIT ACCESSION NO.
11. TITLE (Include Security Classification) AUTOMATIC DATA RETRIEVAL FROM ROCKET MOTOR HOLOGRAMS						
12. PERSONAL AUTHOR(S) Orguc Emin Sami						
13a. TYPE OF REPORT Master's Thesis		13b. TIME COVERED FROM _____ TO _____		14. DATE OF REPORT (Year, Month, Day) 1987 December		15. PAGE COUNT 55
16. SUPPLEMENTARY NOTATION						
17. COSATI CODES			18. SUBJECT TERMS (Continue on reverse if necessary and identify by block number)			
FIELD	GROUP	SUB-GROUP	→ hologram, image analysis, speckle, ImageAction Itext/PC, STATGRAPHICS <i>solid Rocket Propellant thesis, Speckle Interferometry</i>			
19. ABSTRACT (Continue on reverse if necessary and identify by block number) This thesis describes a technique of obtaining particle size information from holograms of combustion products. These data are needed to improve predictive capabilities of propellant performance, to provide input related to ammonium perchlorate (AP) - aluminum interactions for steady-state combustion models and to provide in motor particle size distributions to allow more accurate predictions of damping in stability analysis and two phase flow and exhaust plume signature. This study describes the use of Itext/PC software for the filtering and processing of the hologram images to reduce speckle and also, improves a Fortran program which had been written before to extract the particle feature size data from the modified image. The final step shows the statistical particle feature data exhibition by using the STATGRAPHICS (Statistical Graphics System) software.						
20. DISTRIBUTION / AVAILABILITY OF ABSTRACT <input checked="" type="checkbox"/> UNCLASSIFIED/UNLIMITED <input type="checkbox"/> SAME AS RPT <input type="checkbox"/> DTIC USERS				21. ABSTRACT SECURITY CLASSIFICATION UNCLASSIFIED		
22a. NAME OF RESPONSIBLE INDIVIDUAL John P. Powers			22b. TELEPHONE (Include Area Code) (408) 646-2200		22c. OFFICE SYMBOL 62Po	

Approved for public release; distribution is unlimited.

AUTOMATIC DATA RETRIEVAL
FROM ROCKET MOTOR HOLOGRAMS

by

Emin Sami Orguc
Lieutenant Junior Grade, Turkish Navy
B.S., Turkish Naval Academy, 1981


Submitted in partial fulfillment of the
requirements for the degree of

MASTER OF SCIENCE IN ELECTRICAL ENGINEERING

from the

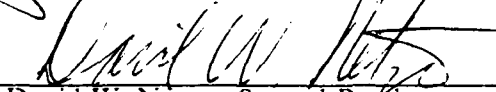
NAVAL POSTGRADUATE SCHOOL
December 1987


Author:



Emin Sami Orguc

Approved by:


John P. Powers, Thesis Advisor


David W. Netzer, Second Reader


John P. Powers, Chairman,
Department of Electrical and Computer Engineering


Gordon E. Schacher,
Dean of Science and Engineering

ABSTRACT

This thesis describes a technique of obtaining particle size information from holograms of combustion products. These data are needed to improve predictive capabilities of propellant performance, to provide input related to ammonium perchlorate (AP) - aluminum interactions for steady-state combustion models and to provide in motor particle size distributions to allow more accurate predictions of damping in stability analysis and two phase flow and exhaust plume signature. This study describes the use of Itex PC software for the filtering and processing of the hologram images to reduce speckle and also, improves a Fortran program which had been written before to extract the particle feature size data from the modified image. The final step shows the statistical particle feature data exhibition by using the STATGRAPHICS (Statistical Graphics System) software.



Accession For	
NTIS GRA&I	<input checked="" type="checkbox"/>
DTIC TAB	<input type="checkbox"/>
Unannounced	<input type="checkbox"/>
Justification	
By _____	
Distribution/ _____	
Availability Codes	
Dist	Avail and/or Special
A-1	

TABLE OF CONTENTS

I.	INTRODUCTION	9
II.	HOLOGRAM IMAGE PROCESSING	12
A.	ACQUIRING THE HOLOGRAM IMAGE	13
B.	SOFTWARE FOR IMAGE ACQUISITION AND ENHANCEMENT	17
1.	Saving and Restoring the Image	17
2.	Filtering	18
3.	Histogram	18
4.	Thresholding	18
C.	PARTICLE DATA EXTRACTION	20
1.	Feature Identification and Labeling	21
2.	Sizing the Features	22
3.	Data Display	23
III.	SPECKLE REDUCTION BY FILTERING	25
A.	SPECKLE AND SPECKLE INDEX	25
B.	THE SPECKLE REDUCTION FILTERS	28
1.	Region-Dependent Segmentation Techniques	28
C.	COMPARISON OF THE FILTERS	33
1.	Comparison of the Speckle Suppression Capability	33
2.	Comparison of the Times Needed per Iteration	37
3.	Visual Comparison and Resolution Degradation	37
IV.	PARTICLE DATA ACQUISITION AND MEASUREMENT RESULTS	40
A.	THE PROCESS BREAKDOWN	40
B.	CURRENT MEASUREMENT RESULTS	41
C.	CONSTRAINTS OF THE PROCESS	49

V. CONCLUSIONS 50
APPENDIX : LIST OF ABBREVIATIONS 52
LIST OF REFERENCES 53
INITIAL DISTRIBUTION LIST 55

LIST OF TABLES

1. TIMES PER FILTER ITERATION. 37

LIST OF FIGURES

2.1	(a) Calibration Test Array Circular Part and Test Pattern (b) Test Pattern Sizes (in μm) and Relative Positions [Ref. 2 pp. 37-38]	14
2.2	USAF Standard Resolution Chart	15
2.3	Hologram Reconstruction [Ref.3 p. 13]	16
2.4	(a) Ideal Histogram [Ref. 3] (b) Real Histogram Representation [Ref. 3]	19
3.1	(a) AFRT without Speckle, (b) Same Image with Speckle	26
3.2	Sample Array used for Template Matching	29
3.3	The template of the Gaussian Filter	30
3.4	(a) Unfiltered Image of the AFRT (SI = 0.8605338) (b) Same Image Filtered with Gaussian Filter (2 iterations, SI = 0.4154431)	31
3.5	(a) Unfiltered and Thresholded Image (b) Gaussian Filtered and Thresholded Image	32
3.6	The template of the 5x5 Convolution Filter	33
3.7	(a) Unfiltered Image of the AFRT (SI = 0.8605338) (b) Same Image Filtered with 5x5 Convolution Filter (2 iterations, SI = 0.1055788)	34
3.8	(a) Unfiltered and Thresholded Image, (b) Convolution Filtered and Thresholded Image	35
3.9	Speckle Index Comparison of the Filters	36
3.10	Comparison of the Resolution Degradation	39
4.1	Particle Distribution of One Field of View in the Calibration Array	42
4.2	Particle Distribution of Seven Fields of View in the Calibration Array	43
4.3	Particle Distribution of Ten Fields of View in the Calibration Array	44
4.4	Particle Distribution of Sixteen Fields of View in the Calibration Array	45
4.5	Particle Distribution of One Field of View in the Real Combustion Hologram	46
4.6	Particle Distribution of Three Fields of View in the Real Combustion Hologram	47
4.7	Particle Distribution of Five Fields of View in the Real Combustion Hologram	48

ACKNOWLEDGEMENTS

I would like to express my deep thankfulness to my thesis advisor, Dr. J. P. Powers, and second reader, Dr. D. W. Netzer, for their numerous suggestions and help that have had a major influence on this thesis.

I am also grateful to all my teachers in my entire education life for the state-of-the-art education.

I. INTRODUCTION

The goal of this thesis, which is a continuation of a research being conducted at Naval Postgraduate School, is to describe a technique for obtaining particle size information from holograms taken of the combustion products in a rocket combustion chamber. The ultimate output of the process is going to be used to study the effects of addition of aluminum and other metallic particles on the performance in solid propellant motors. The main benefit of adding the aluminum is to suppress high frequency combustion instabilities and to increase the delivered performance. The other metallic additives are generally added only to increase the acoustic stabilization in reduced-smoke propellants. These are a small amount of aluminum oxide, zirconium, etc. The particle size distribution has a major effect on the performance throughout the rocket motor and nozzle [Ref. 1]. Direct observation is the most effective method to get the information about particles and to evaluate the existing analytical methods, because no data exists which will permit the prediction of the distribution of the particle sizes in the combustion chamber of the motor.

Holographic techniques, which have been used to record the dynamics in the combustion chamber, are still to be improved. This is accompanied by improvements in the taking and processing of holograms. Previous work done in processing the images have included the use of an IBM PC/AT with special software and hardware [Ref. 2] and an attempt to reduce speckle noise by applying some nonlinear filters (the Sigma filter, the Geometric filter and the Local Statistical filter), which were taken from the synthetic aperture community [Ref. 3].

In Reference 2, Redman focussed on image capture, image digitization and particle sizing of the holograms. ImageAction software from Imaging Technology, Inc., was used under operator control to process the image, and to suppress the speckle effect. Locally developed Fortran programs were then used to process the images and to size the particles. Due to computation time and computer memory size constraints, Redman's efforts worked with only one quarter of the screen image (256 x 256 pixels). A major problem was that the processing time for the one quadrant of the screen was taking approximately 4 hours.

In an attempt to reduce the speckle effect, Redman also investigated image averaging techniques. One method used a spinning mylar disk to blur the speckle background during the integration time of the imaging tube. Another used a digital averaging of several captured images. It was found that the spinning mylar disk was optimal to reduce the speckle in that the same amount of speckle reduction could be done in a simpler fashion than the digital averaging. The digital averaging technique was abandoned in later work. The speckle was further reduced by using some built-in routines of the ImageAction software. First, a blur filter was applied followed by a lowpass filter. The two-step process was then repeated until the filtered image satisfied the user's needs. When the correct filtering was done, the speckle was significantly reduced. It was noted, however, that resolution was also reduced and that close particles would tend to merge into one unresolved clump after processing. No attempt was made to quantize the loss of resolution in this early work. The next processing step was the application of a threshold to remove all information from the background. The thresholded image was then processed by the Fortran routines for object identification, counting and sizing. Twenty microns was the best resolution that could be achieved using these speckle reduction techniques and computer processing.

This thesis improves the previous work both in reducing the speckle noise by trying some locally developed filters (the 5x5 Convolution filter and the 3x3 Gaussian filter) and in developing a Fortran program that reduces the time for extracting the feature size. Feature data extraction programs can be run almost 100 times faster now. It takes about 10 minutes to process the entire visible monitor screen image instead of 4 hours for one quarter of the screen required in the previous study. Furthermore, it was observed that although the locally developed filters do not provide any significant improvement in terms of reduction of the speckle compared to the previously developed nonlinear filters of Ref. 3, they can be run much faster. Additionally the work for this thesis suggests that the histogram of the particle size distribution reaches a representative shape after summing information from a sufficient amount of particles (approximately 1,000 particles). Further study is needed to verify this initial observation.

This thesis consists of six chapters. The first section of Chapter Two provides some background material to explain the process for acquiring the hologram images and the software used for processing the image. The second section explains the steps of the data extraction process and the details of the algorithm. Chapter Three, at the

beginning, gives a description of *speckle* and *speckle index*, a parameter used to determine how much speckle is present. Other sections provide the definitions of the two locally developed filters (the 5x5 Convolution filter and the 3x3 Gaussian filter) and compares these filters with previous nonlinear filters (the Local Statistical filter, the Geometric filter, the Sigma filter). Chapter Four gives a brief description of the steps for the feature identification and sizing process and evaluates the performance of the process. Furthermore, current measurement results are given in this chapter. The concluding remarks are included in Chapter Five.

II. HOLOGRAM IMAGE PROCESSING

As mentioned in the previous chapter, holographic techniques are used to capture the image of the combustion products in a rocket combustion chamber during firing. The pulsed ruby laser utilized in the recording process uses a glass diffuser in its illumination path. This diffuser is necessary to cut down the presence of schlieren interference fringes produced by the thermal and density gradients surrounding the burning particles in the rocket motor [Refs. 4,5].

The hologram is then reconstructed using a krypton laser and viewed through the microscope using 2x, 4x or 10x magnification. The diffuse light from the recording interferes with the reference wave of the krypton reconstruction laser. This random interference causes speckle to be introduced into the image. By attaching a 0.5 lux low-light-level camera and a video cassette recorder to the microscope, the speckle-corrupted image is recorded and preserved for later use. Explanation of the reconstruction process is described in more detail in the next section.

After the reconstruction of the hologram, the entire image processing and feature extraction process is done with an IBM-PC/AT microcomputer. Basically, the hardware and software requirements for the system can be summarized as following.

1. PC Vision frame-grabber board (installed on the IBM-PC/AT),
2. ImageAction and Itex PC software (both by Imaging Technology),
3. An analog video monitor,
4. A video cassette recorder, and
5. Graphics software (STATGRAPHICS).

Recently, the computer system has been upgraded with a 16 MHz. 386 microprocessor board. This board has provided significant improvement in processing speed.

Three test objects have been used in the phases of study. Two of these objects were imaged under white light as the highest contrast for the calibration purposes. They were also recorded as holograms in the test setup to duplicate the test geometry.

The first object was a calibration reticle produced by LEOS, Inc. It is a test pattern and consists of twenty three standard sizes ranging from five to ninety-three microns in diameter. Circle sizes and relative positions of the test array and pattern

are as shown in Figure 2.1. Approximately 10,000 photodeposited spots form the circular portion of the reticle. The diameter of the circular part is almost eight millimeters. The object contains an extra test pattern at its right side showing the sample sizes of the particles. The circular part can be used to obtain the particle distribution and statistics to calibrate the speckle reduction methods. Also, the test pattern can be used to coarsely measure the resolution sensitivity and speckle reduction capability of the method.

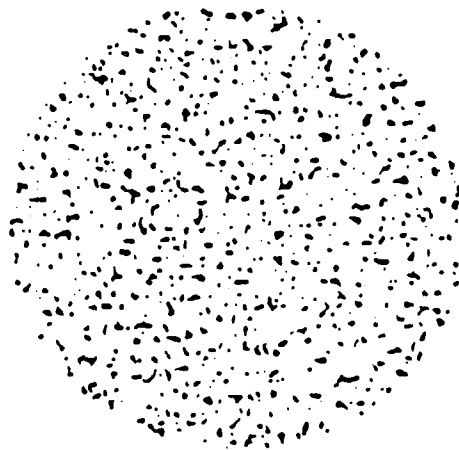
The second object of study was the 1951 USAF Standard Resolution Chart. This was used for resolution degradation comparison of the filters, because it provides more continuous and sensitive measurement of resolution degradation than the LEOS calibration array (Figure 2.2).

The final objects were the reconstruction images obtained from rocket motor holograms recorded during firing using fuel samples supplied by the Air Force. They were used for the ultimate goal of the investigation, to obtain the feature distribution and statistics of the particles in actual combustion conditions. Comparison and relations between the images obtained from the calibration array and the rocket motor holograms are presented in Chapter Five.

A. ACQUIRING THE HOLOGRAM IMAGE

The holographic techniques that are used to capture the image of the combustion products in a rocket combustion chamber during firing and the reconstruction process of this image have been described in detail in Reference 1 and 2.

The hologram reconstruction scheme is shown in Figure 2.3. Basically, the hologram is reconstructed using a Krypton laser (whose wavelength is close to that of the pulsed ruby laser used to record the hologram) and viewed through the microscope. The spinning mylar disk is another key part of the system, because the focussing image on the spinning mylar disk was found to reduce the speckle [Ref. 3: p. 39]. The low transmissivity of the mylar disk causes a reduction of the light at the input of the camera. Therefore, a 0.5 lux low-light-level camera was attached to the system. Then, by attaching a VCR to the camera, the speckle-corrupted image can be recorded and preserved for later use. During the reconstruction phase, the random interference between the diffuse light from the recording and reference wave of the krypton reconstruction laser produces the speckle which has proven to be one of the main problems of the feature extraction.



(a)

9	7	5		
27	24	21	17	12
43	40	37	34	31
61	56	52	50	47
93	87	81	74	67

(b)

Figure 2.1 (a) Calibration Test Array Circular Part and Test Pattern
(b) Test Pattern Sizes (in μm) and Relative Positions [Ref. 2 pp. 37-38].

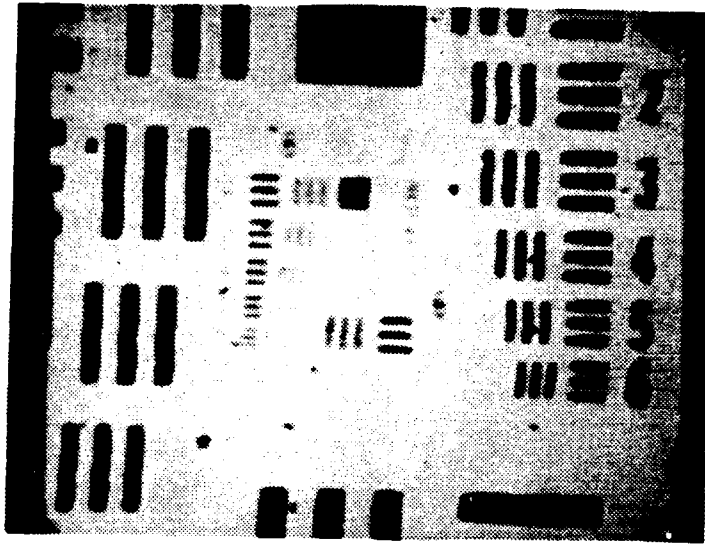


Figure 2.2 USAF Standard Resolution Chart.

In the reconstruction process, the field of view (and the number of particles within that field of view) is determined by the magnification required to resolve the smallest particle. For each magnification power of the microscope, each pixel has a different fixed size. The particle size is measured in terms of pixels. This leads to a quantization error for those particles that are not exactly an integer number of pixels. It is not yet understood how the TV camera tube quantized the image edge (i.e., whether it rounds up, rounds down, or uses some other truncation scheme). In any event the edge is resolved to ± 1 pixel. For a small object this uncertainty is a large fraction of the image size. For a large object, the uncertainty of size is negligible.

The physical size of a pixel is determined by including a calibration object of known dimensions within the hologram volume. The combustion holograms included a screw profile. The known pitch of the screw is used to find the pixel dimensions.

The 4x magnification proved to provide a reasonable processing time for one particle in one field of image with a smallest feature size of 3.7 microns. This can be described as the quantization step size of particle resolution measurement. For example, the smallest particle in the LEOS calibration array is 5 microns. An uncertainty of ± 3.7 microns would lead to significant error if these particles were

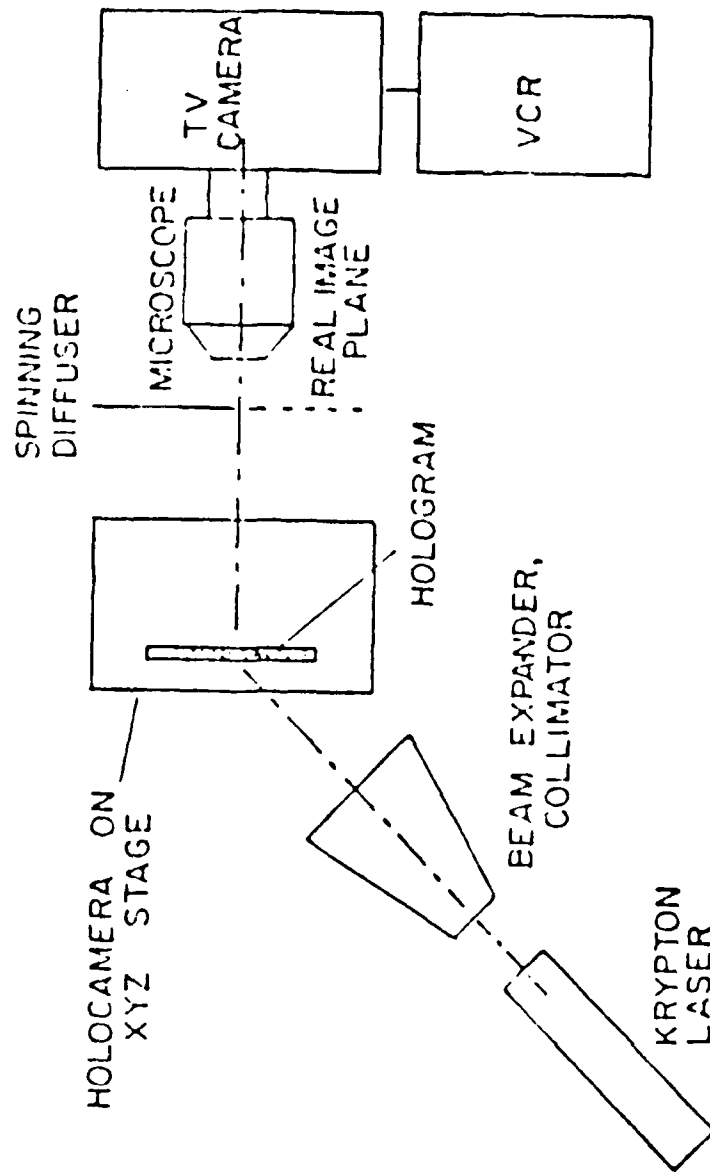


Figure 2.3 Hologram Reconstruction [Ref.3 p. 13].

resolved. The same error for a 17 microns (or greater) particle is tolerable for our initial measurements. A 10x magnification would improve the quantization error effects, but there would be fewer particles in the field of view thus requiring more computation time for the hologram volume. This is a fundamental tradeoff between acceptable quantization error and computation time. The magnification of 4x proved to be an acceptable compromise value.

B. SOFTWARE FOR IMAGE ACQUISITION AND ENHANCEMENT

As was discussed in previous studies [Refs. 2,3], the ImageAction and IteX PC commercial software were the key elements of the entire process. This software permits the user to process either the entire monitor screen or just some portion of it. The user can describe any rectangular portion of the monitor screen as an Area of Interest (AOI). It is possible to process an entire image which is made up of 512 x 480 pixels on the monitor screen, since last 32 rows of the monitor cannot be seen. More detailed technical information about this software are available in the documentation [Refs. 6,7]. Now, some aspects of this software can be discussed in a general overview.

1. Saving and Restoring the Image

Both ImageAction and IteX PC have the capability of saving the processed images and using the same images by restoring later. Menu-driven ImageAction subroutines or locally prepared user programs that call the IteX PC subroutines provide this flexibility. Some subroutines were developed for saving and restoring the images in References 2 and 3, and they were also used during this phase of the investigation. Normally each stored image in a file has 64 bytes of header and 32 bytes of comment following this header. Then 256,144 bytes are used to store the entire image screen. Loading the images from the hard disk of the computer will save time over transferring the image from a floppy disk. It takes almost 10 seconds to transfer the image from a hard disk to the video screen, while twice that time is needed to transfer the image from the floppy disk drives.

Another important detail is that an image file saved by the IteX PC or ImageAction softwares is an ASCII string file and may not be compatible with any other software's data format. Some compilers such as Fortran can have problems handling this kind of string file. A sample conversion program that read the data and rewrote it in compatible form was written in Basic by Redman [Ref. 2: p. 66] for the use of a Fortran compiler.

2. Filtering

Filtering is the most important step of speckle reduction techniques. Most speckle reduction techniques use simple convolution techniques. Detailed information about some of the speckle reduction filters are in the previous studies [Refs. 3,5,8,9,10].

The ImageAction and IteX/PC software have many methods of image filtering and enhancement (3x3 Gaussian filter, 5x5 Convolution filter, 7x7 Convolution filter, Blurring, Sharpening, etc.). Every filter has the disadvantage of tending to blur or smear the actual particle shapes resulting in some loss of edge resolution. In part of the study for this thesis, the Gaussian filter and the 5x5 Convolution filter of this software were evaluated for speckle reduction capability and resolution protection. This evaluation and the comparison of these filters with the other nonlinear filters like the Geometric filter, the Sigma filter and the Local Statistical filter [Ref. 3: pp. 33-36] are discussed in the next chapter.

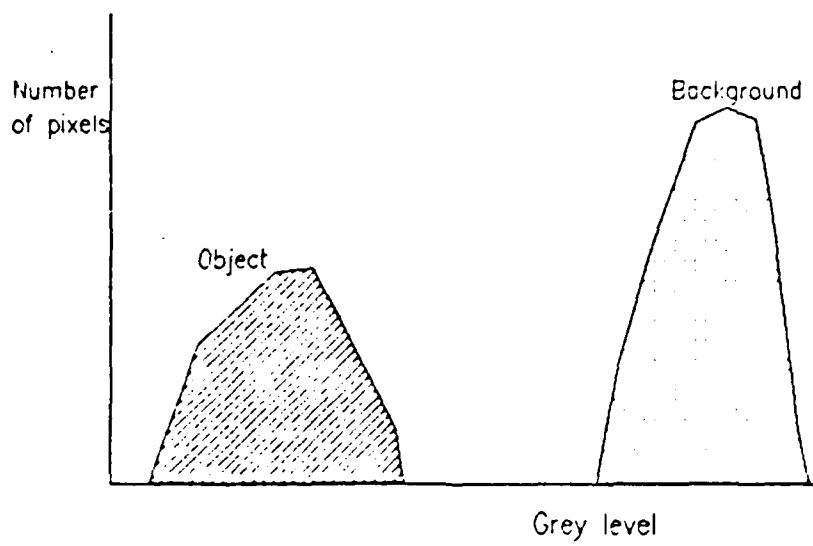
3. Histogram

An image histogram is a plot of the number of pixels having a given value of gray level versus the value of the gray level. A good decision of the location of a threshold can frequently be made after looking at the histogram of the image to differentiate the features from the background. Also, the histogram of an hologram image gives a general idea about the population of the particles on the background. ImageAction and IteX/PC have some subroutines to obtain the histogram of the image, and to display it on the screen. But, since there is no any capability of getting the hardcopy of the output, STATGRAPHICS software was used for this purpose during the study.

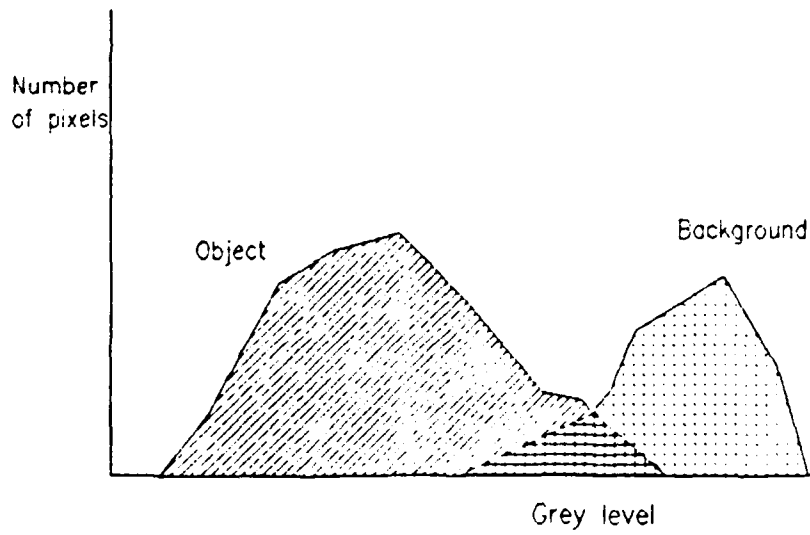
4. Thresholding

Thresholding is a process to set the pixels of the particles and the pixels of the background to two different values. As can be seen in the ideal case (Figure 2.4), there is no overlap area between the particles and the background. A threshold set between the regions will produce black particles on a white noise-free background. However, in an actual image, the particles and the background are going to overlap each other as in Figure 2.4. No matter where a threshold is placed, there are going to be errors while evaluating the image.

Selection of the threshold value is going to play the main role on the amount of error created by the crossover area. During this study, the threshold value is determined by direct observation of the processed image, and the effectiveness of the



(a)



(b)

Figure 2.4 (a) Ideal Histogram [Ref. 3]
(b) Real Histogram Representation [Ref. 3].

decision is going to depend on the experience of the user observing the particles. In each case, as a probabilistic conclusion, there will be some speckle described as a particles below the threshold. Naturally, it is obvious that some particles will be evaluated as a speckle and lost.

A threshold subroutine was written by Edwards [Ref. 3: p. 43]. This subroutine uses the IteX/PC subroutines and has only one threshold limit. The pixel values below the threshold will be changed into zero value (black), and the others into level 255 (white). The PC Vision image memory board will preserve the original image until the thresholded image is mapped which is an additional user operation. This provides a chance to the user to try the various values of the threshold before deciding which is best.

Proper filtering and other enhancement techniques are required to help separate the particles and background lobes before applying a threshold, and so to decrease the overlap area.

C. PARTICLE DATA EXTRACTION

The main goal of this study was to improve a computer-aided system which is capable of measuring the quantity and the size of solid particles from holograms made of the combustion products in a combustion chamber of a rocket motor. Redman [Ref. 2] built the basics of this kind of measurement, but the previous study had some technical constraints.

The two most important desired improvements were to reduce the time to process the image, and to process the entire monitor screen image (512 x 512). Redman's study was limited to 256 x 256 images and required almost four hours processing time for this image. Significant effort was spent to improve the speed and the efficiency of these programs. Now, 512 x 480 (visible full screen) images can be handled in approximately 10 minutes from frame digitization to the production of the feature data table. Improvements have been due to commercial availability of software that manipulates the fast-access video memory board (VMB), improved software revisions on locally produced programs, and the addition of a faster microprocessor.

The revised program has been written in two sections in Fortran. The modular structure allows the user to easily test each segment. The first section of the program counts the number of features and codes each individual feature as a unique number in sequential order. The second section of the program sizes the features in terms of area and diameter. The expected sizes of the particles range from one micron to 200 microns in diameter. They are also be expected to be nearly spherical in shape.

1. Feature Identification and Labeling

The feature identification and labelling part of the algorithm requires the thresholded image. In the thresholded image, the features are coded into pixel value '0' (black) and the background is coded into pixel value '255' (white). The thresholded image is then loaded into the feature identification and labelling program.

The feature identification and labelling program consists of three phases. In the first phase, the program sweeps the image row by row moving from left to right. It reads each pixel by using ITEX PC subroutines. If the pixel value is '255', this pixel is skipped. When the program meets a '0' value the first time, this pixel is labelled a unique feature number contained in a sequential counter. The counter value represents a temporary feature number and can range from '1' to '254'. The program then continues to check the other pixels in the described order (row by row moving from left to right). When the program meets another '0' value, first the algorithm checks the previous pixel in the same row. If the previous pixel has a feature number, the current pixel is labelled with the same feature number, and the program continues to check the next pixel. If the previous pixel is a '255' background pixel, the program checks the pixel above the current pixel. If that pixel (above the current pixel) has a feature number, the current pixel is labelled with the same feature number of the pixel above it. The program then continues to check the next pixel. But, if that pixel (above the current pixel) is a '255' background pixel, the program seeks a connection between the current pixel and the right-upper diagonal pixels, one row above the current pixel. First, the algorithm checks the next pixel in the same row as the current pixel. If the next pixel is a '255' value, the program assigns a unique sequential feature number to the current pixel. (In that case the current pixel and the diagonal pixel can not belong to the same feature.) If not, the algorithm checks the pixel above the next pixel. (That pixel is the right-upper diagonal pixel of the current pixel.) The purpose of checking the next pixel value in the same row instead of checking the right-upper diagonal pixel value directly is to be sure that the current pixel and the diagonal pixel belong to the same feature. When the algorithm meets a feature pixel on the right-upper diagonal direction, the current pixel is labelled with the diagonal pixel's value. But, if the diagonal pixel is not a feature pixel, the other pixels to the right of the right diagonal are checked with the same logic. (The check continues until a row end is reached.) When the program meets a feature pixel, it assigns this diagonal feature value to the current pixel. Otherwise, the program labels the current pixel with a

unique sequential feature number. As a result of this algorithm, some feature geometries can produce features that have pixels that have different feature values.

At the second phase of the program, all pixels of each feature are assigned the same feature value and each feature will have a pixel assignment. Before starting the second phase, the program asks the user for the maximum length of the largest feature on the current monitor screen. The user gives an approximate answer for this question in terms of pixels. A typical value is seventy. This length is going to describe a square window to enclose the largest particle on the screen. The larger the value given, the longer the program takes to run as the loops truncate at the maximum estimated particle size.

Once all the particles have been labelled as described in the first phase, the program performs the second phase in a fashion similar to the first phase. This time, it tests each pixel with the one above it. The sweeping direction is column by column moving from top to bottom. If there is a mismatch between the feature's pixel values (except the background pixels), it assigns the previous pixel's value to the one below it, and to the other adjacent pixels following it that have the same value. Each time, this process is done in the window described above. At the end of this phase, there will generally be some gaps between the values of the features, because of the pixels which have the values reassigned and the feature values cancelled.

In the third phase, the features on the image are arranged in sequential order. First, the count register is reset. Then the program sweeps each row again. When it finds two features having feature numbers not in sequential order, the algorithm substitutes the sequential value.

When finished, each feature on the current screen is assigned a unique feature number from 1 to a maximum of 254. If there are more than 254 particles on the screen, they are also assigned the values like the others between 1 to 254, but they are differentiated with a special group count register. The group count register is increased by one for each new group. This restriction of 254 particles exists, because the gray levels of the pixels are represented with the values between 0 and 255 in the Itex PC software.

2. Sizing the Features

The second module of the locally produced program is to find the specific dimensions of the features. This part uses the images labelled in the previous module, and finds the horizontal and vertical diameters of the particles. It also finds the total area of the particles. All measurements are in units of microns.

First, the program asks for the number of features on the screen. This was displayed on the screen as an output of the previous module that identified and labelled the features. This value should be saved as a comment if the user chooses to store the labelled image. The program will save the value supplied by the user in a feature count register and count down as it finds the dimensions of each particle. Another question from the program is the magnification used with the microscope. This is necessary for the calculation of the dimensions in microns. As can be seen, larger magnifications will affect the minimum particle resolution. For example, the resolution of the minimum particle which is covered just one pixel on the screen is going to be 3.7 microns for the magnification of 4x. The real size of one pixel on the current screen is calculated by a calibration object image, and duplicated for the images which have known magnifications.

The last thing before running the program is for the user to enter the maximum length of the biggest particle. It is obvious that this will be the same as it was in the identification and labelling program.

The program tests the pixels row by row from the left-upper corner to the right-lower corner. Whenever the algorithm meets a labelled feature, it builds the local window around it. Then, in this window, the program counts the pixels carrying the same number as the feature count register. The summation gives the area of the particle. It goes through this window twice and calculates the vertical and horizontal diameters of the feature. As a final step, it changes the pixel values of the feature to the '0' (black particle) and decreases the feature count register by one. Then, the program continues sweeping the rows checking each pixel. Black '0' and White '255' pixels are skipped. Concurrently, six separate registers test the measured dimensions of the features to find the maximum and minimum particles on the current screen. At the end of the process, the program creates an output file to transfer and to process them in the STATGRAPHICS program. This table lists the feature identification number, the feature area, the feature's x-width, and the feature's y-width.

3. Data Display

Exhibition of the feature data is the last step of the process. The STATGRAPHICS software was selected as a compatible graphics system. The reason for selecting the STATGRAPHICS software was its user friendly structure and its compatibility with the IBM-PC/AT. Furthermore, it has good capabilities to exhibit the statistical data features.

STATGRAPHICS imports the output data file of the previous program by using its *Data Management Utilities*. The details are summarized in Chapter Four. The STATGRAPHICS program has a capability of exhibiting the results in a table or in a histogram. Each data display selection has other alternatives such as relative or cumulative distribution, etc. Furthermore, the program has the capability of adding the data files cumulatively allowing the user to see the statistics of more than one field of a histogram. At the end, the user can take a hardcopy of the entire study.

III. SPECKLE REDUCTION BY FILTERING

In Reference 3, Edwards implemented three nonlinear speckle reduction filters (the Geometric filter, the Sigma filter and the Local Statistics filter), and compared the performances of these filters in terms of speckle index reduction, visual differences, timing constraints and histogram differences. These filters had already been designed by the SAR (Synthetic Aperture Radar) community [Refs. 8,9,10]. The conclusion of the previous study was that the Geometric filter was found to be the best overall filter [Ref. 1: p. 39]. But, the times needed for one iteration of these filters were still too much. For example, the fastest of them, the Sigma filter needs about 2.5 minutes per iteration for a full monitor screen. One iteration takes about 6 minutes for the Geometric filter, and 13 minutes for the Local Statistics filter. Since four to six iterations are typically required, significant amounts of time can be spent in reducing the speckle using these filters. Therefore, in this part of this investigation, some locally developed filters (5x5 Convolution filter and 3x3 Gaussian filter) were tested. Actually, they use simple convolution techniques. As can be seen at the later parts of the discussion, the locally developed filters are much faster than the nonlinear filters, but they have worse resolution degradation performance.

Before starting the introduction and the performance comparison of the filters, it will be helpful to describe the speckle and speckle index.

A. SPECKLE AND SPECKLE INDEX

During the construction process, all holograms are recorded with diffuse illumination from the laser. This is done in order to minimize the presence of schlieren interference fringes produced by temperature and density variations of the combustion gas products during the burn. A glass diffuser produces the diffuse illumination in the illumination beam. This diffuse illumination creates the speckle effect in the reconstructed images [Ref. 4: p. 2]. The presence of the speckle reduces the ability of a human observer to resolve the detail. The effect of the speckle can be seen easily in Figure 3.1. The bottom part of the figure shows the speckle overlaying the features of the non-speckle image of the top part. Since the speckle can have a maximum size that is comparable to the smaller particles, smaller feature particles can easily be confused with the speckle. Therefore, the speckle creates the major problem in the feature extraction from holograms.



(a)



(b)

Figure 3.1 (a) AFRT without Speckle,
(b) Same Image with Speckle.

Speckle has been described as having the characteristics of a random multiplicative noise in the sense that the noise level increases with the average gray level of a local area [Ref. 10: p. 636]. In theory, it is known that the intensity of speckle has a shape of a negative exponential distribution. However, in practical applications, it is quite difficult to describe a proper model. Basically, the SAR community proposed two major categories of the speckle-suppression techniques. The first category includes the averaging of multi-frames. This will help reduce the noise variance. Redman found that recording the image off a spinning mylar disk had the same effectiveness as averaging the multi-frames, and was accepted as optimal in both speckle reduction and in processing time [Ref. 2: p. 42]. Techniques in the second category smooth the speckle after images have been reconstructed. To filter the speckle from the images requires a precisely defined statistical property, such as correlation between neighboring pixels and the standard deviation. Various filters belong to this post-image category. The important problem is the tendency of the filters to suppress the desired shapes as well as its speckle. This is known as the resolution degradation of the filter.

The major indicator evaluating the speckle reduction capability of the filters is *speckle index* described by Crimmins [Ref. 8: p. 651]. The algorithm proposed by Crimmins was the following:

The local deviation is defined as

$$\sigma(m,n) = \max \{F(m+a,n+b)\} - \min \{F(m+a,n+b)\} \quad (3.1)$$

$$-1 \leq a,b \leq 1$$

and the local mean is

$$\mu(m,n) = \frac{1}{9} \sum_{a,b=-1}^1 F(m+a,n+b) \quad (3.2)$$

The speckle index is then defined by

$$\text{speckle index} = \frac{1}{MN} \sum_{m=1}^M \sum_{n=1}^N \frac{\sigma(m,n)}{\mu(m,n)} \quad (3.3)$$

The speckle index gives the ratio of the standard deviation of the image sector to the mean of the pixel values in a definite local region. A Fortran subroutine computing the speckle index was written by Edwards [Ref. 3: pp. 41-42]. The same subroutine was used to evaluate the performances of the filters developed for this thesis.

In the equations above, M and N are the dimensions of the local area in which the speckle index was calculated, and $F(m,n)$ represents the image in terms of the gray level of each pixel. Values of M and N were selected as 240, since it was found by Edwards [Ref. 3: p. 19] to be a reasonable value.

B. THE SPECKLE REDUCTION FILTERS

As mentioned in the previous section, in addition to the nonlinear filters some other filters based on basic convolution techniques were evaluated in terms of speckle suppression effectiveness. The most important difference between convolution techniques and nonlinear algorithms is that the nonlinear filters have been implemented to suppress the speckle based on a multiplicative noise model, whereas the convolution algorithms are a type of region-dependent segmentation tools.

Before starting the discussion of these special filters, there is a need to consider the fundamentals of the convolution algorithms.

1. Region-Dependent Segmentation Techniques

For the region-dependent algorithms, a region may be considered as an area which is finite and is surrounded by a closed edge [Ref. 12]. Generally, the differences in gray level content are the major tools to establish the region characteristics in visual images. The other important feature which may be used for this purpose is *texture*. Texture can be described as a global repetition of a basic pattern in a local area. This is mostly helpful to identify the edges.

Basically, the convolution algorithms use a *template* (also called a *mask* or *window*). A template is a two-dimensional array which is designed to detect the invariant properties of a region. This method is used widely by the image processing community, because of its simplicity.

An example showing the fundamentals of the *template matching* might be helpful to understand the idea better. Let us consider an image which has a background with a constant gray level, and some isolated particles located in this background with a different gray level. Now, let us take a sample template in 3×3

-1	-1	-1
-1	8	-1
-1	-1	-1

Figure 3.2 Sample Array used for Template Matching.

dimensions and assign some coefficients for each location [Figure 3.2]. This specific array is also known as a *Laplacian Convolution* [Ref. 7: pp. 9-19]. The center position of the template (assigned 8) is shifted around the image from pixel to pixel. At every position, the gray levels of the image which correspondence to the template locations are multiplied with the array coefficients. Then, each local product is added to the others and the value of the sum is stored in an array at a location corresponding to the center of the template. If all image values covered by the template area belong to the background (constant gray levels), the sum will be zero. But, if there is a particle under the template area, the sum will be different from the zero. The summation will be maximum when the particle is located under the center position of the template. For other positions of the particle, the sum will be smaller. Depending on the preferences of the user, the proper threshold application will eliminate these smaller values. By assigning the coefficient values in various ways, it is possible to have many configurations to segment the special properties of the images in the desired directions [Ref. 12: pp. 335-345].

a. 3x3 Gaussian Filter

This filter is a function in the Itext/PC library, and performs an approximate convolution on a local area. The user can select the Area of Interest (AOI) to be either a full monitor screen, a quadrant of the screen or some portion of the screen. The filter essentially tends to blur the image by selectively passing only low spatial frequency components. The algorithm is automatically scaled by pre-set values [Ref. 6: p. II-6-5]. The kernel used for the Gaussian filter is in Figure 3.3.

For illustration of the 3x3 Gaussian Filter's effectiveness, images of the AFRT were used. Figure 3.4 shows an image before and after two iterations of the filter. Visually, the speckle has been reduced a small amount, and the blurring and resolution degradation effects are very small. After the proper thresholding, the

1	2	1
2	4	2
1	2	1

Figure 3.3 The template of the Gaussian Filter.

filtering effect is more obvious. As can be seen in Figure 3.5, good data can be retrieved from the filtered image, whereas the excessive speckle in the unfiltered image would lead to faulty feature detection.

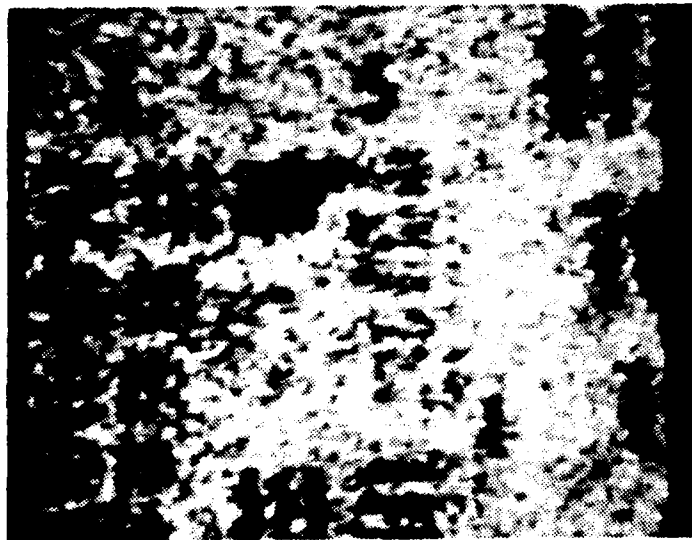
The Gaussian filter can be used as a fast smoothing algorithm. It takes almost 18 seconds to filter the full screen image. But, the speckle suppression is minimal. This is explained at the next section. The Gaussian filter is a general purpose segmentation algorithm, not a special speckle suppression algorithm. Since it does not use any analytical model for the speckle noise in its design, the filter treats the speckle like a particle, and has the same smoothing effect on both speckle and particles. Resolution degradation of this filter is rather good compared with the previous implemented filters like the Geometric, the Local Statistics and the Sigma filters.

b. 5x5 Convolution Filter

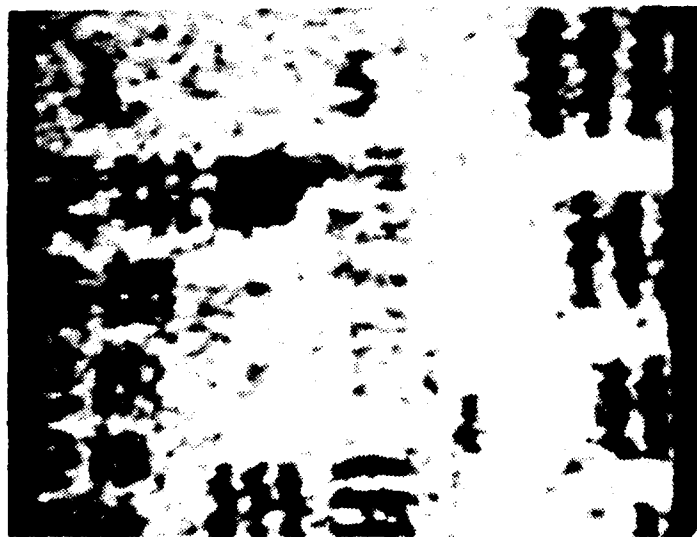
This function performs a 5 by 5 convolution process on a predescribed local area [Ref. 6: p. II-6-3]. This algorithm usually produces a cleaner (i.e., less noisy) enhanced image than 3x3 Gaussian filter, but it takes a bit longer time to run (about 50 seconds for the full screen). The kernel used for the Convolution filter is in Figure 3.6.

During this investigation, the *data scale factor*, which is needed to balance the convolution filtering effect, was selected as 6, and a *data offset* value was selected between 50-60, up to the average gray level of the selected image. The *data scale factor* and *data offset value* are required parameters for the Convolution filter algorithm by the ImageAction software [Ref. 6: p. II-6-4].

The effectiveness of the 5x5 Convolution filter can be seen easily on the AFRT [Figure 3.7]. Visually, the speckle has been reduced considerably, but blurring and resolution degradation effects are much more obvious than for the Gaussian filter.

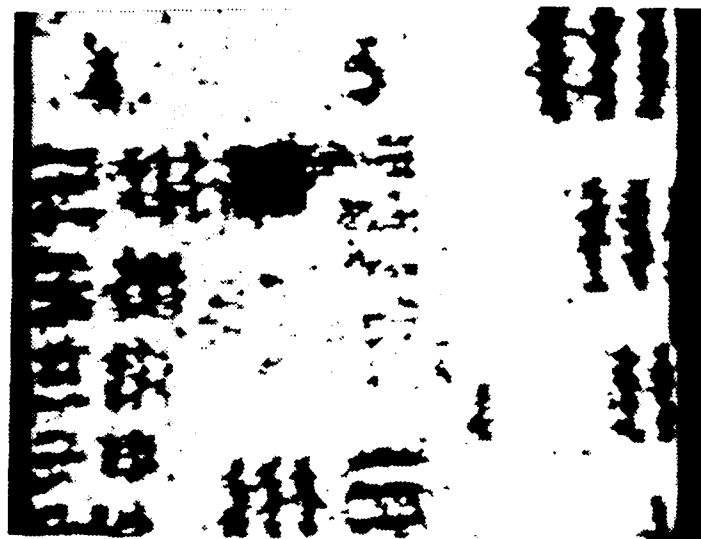


(a)

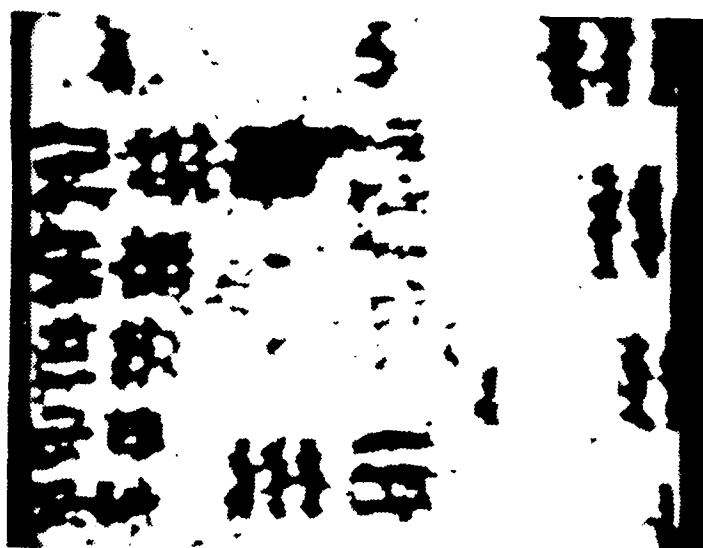


(b)

Figure 3.4 (a) Unfiltered Image of the AFRT (SI = 0.8605338)
(b) Same Image Filtered with Gaussian Filter (2 iterations, SI = 0.4154431).



(a)



(b)

Figure 3.5 (a) Unfiltered and Thresholded Image
(b) Gaussian Filtered and Thresholded Image.

0	1	1	1	0
1	3	3	3	1
1	3	5	3	1
1	3	3	3	1
0	1	1	1	0

Figure 3.6 The template of the 5x5 Convolution Filter.

The speckle suppression effect of the filter is more obvious after applying the proper threshold value on the filtered image. As can be seen in Figure 3.8, the 5x5 Convolution filter is much more effective at clearing the noise, but it also removes some small particles in the image. Concurrently, edges of the retrieved particles spread more than for the 3x3 Gaussian filter.

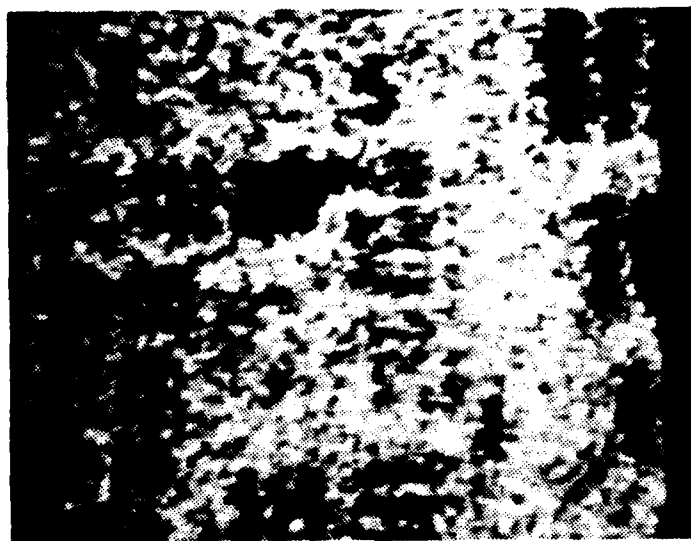
This filter also does not contain any analytical noise model for the speckle, and is a general purpose region dependent segmentation algorithm. The speckle suppression effect is as good as the Sigma filter, but the resolution degradation effect is the worst among all of the filters. These evaluations are exhibited in the next section with numerical values.

C. COMPARISON OF THE FILTERS

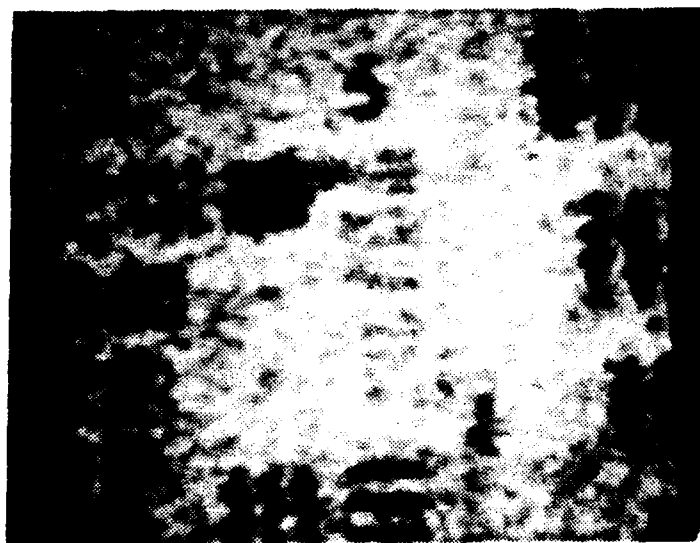
In this section, the two recently developed filters and the three nonlinear SAR filters will be compared in terms of speckle index reduction, the time needed per iteration, and their resolution degradation. For the three nonlinear filters, these comparisons were done before [Ref. 3: pp. 33-36]. To make the comparison from the same reference, the same standards and subroutines were used exactly. Then, the previous results and current results were combined.

1. Comparison of the Speckle Suppression Capability

Comparison of the speckle-suppression capability of the filters is done in terms of the speckle index. As can be seen in Figure 3.9, the Geometric filter, the Local Statistics filter, the Sigma filter and the Convolution filter are approximately equally successful in reducing the speckle after four or more iterations. The Gaussian filter

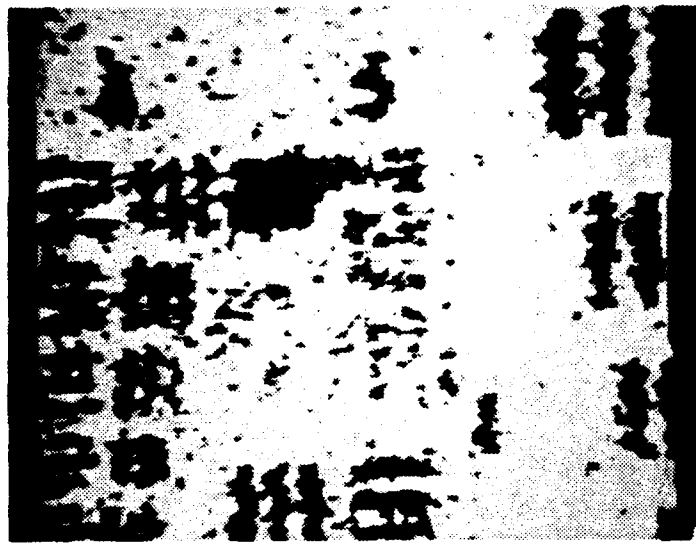


(a)

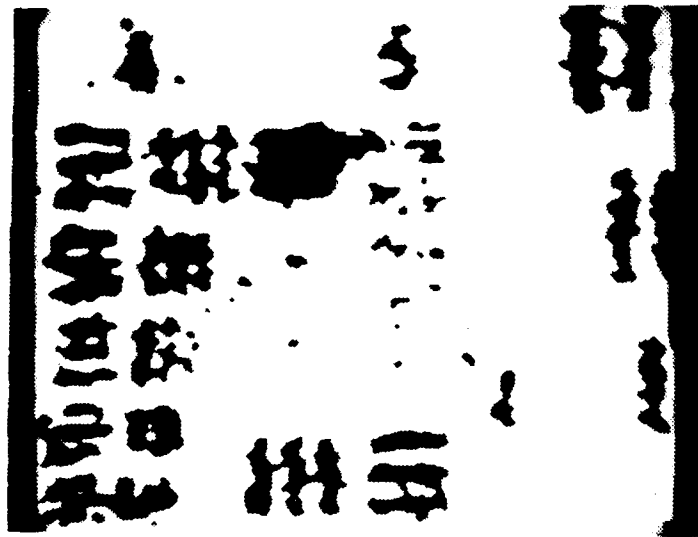


(b)

Figure 3.7 (a) Unfiltered Image of the AFRT (SI = 0.8605338)
(b) Same Image Filtered with 5x5 Convolution Filter (2 iterations, SI = 0.1055788).



(a)



(b)

Figure 3.8 (a) Unfiltered and Thresholded Image,
(b) Convolution Filtered and Thresholded Image.

COMPARISON OF THE FILTERS

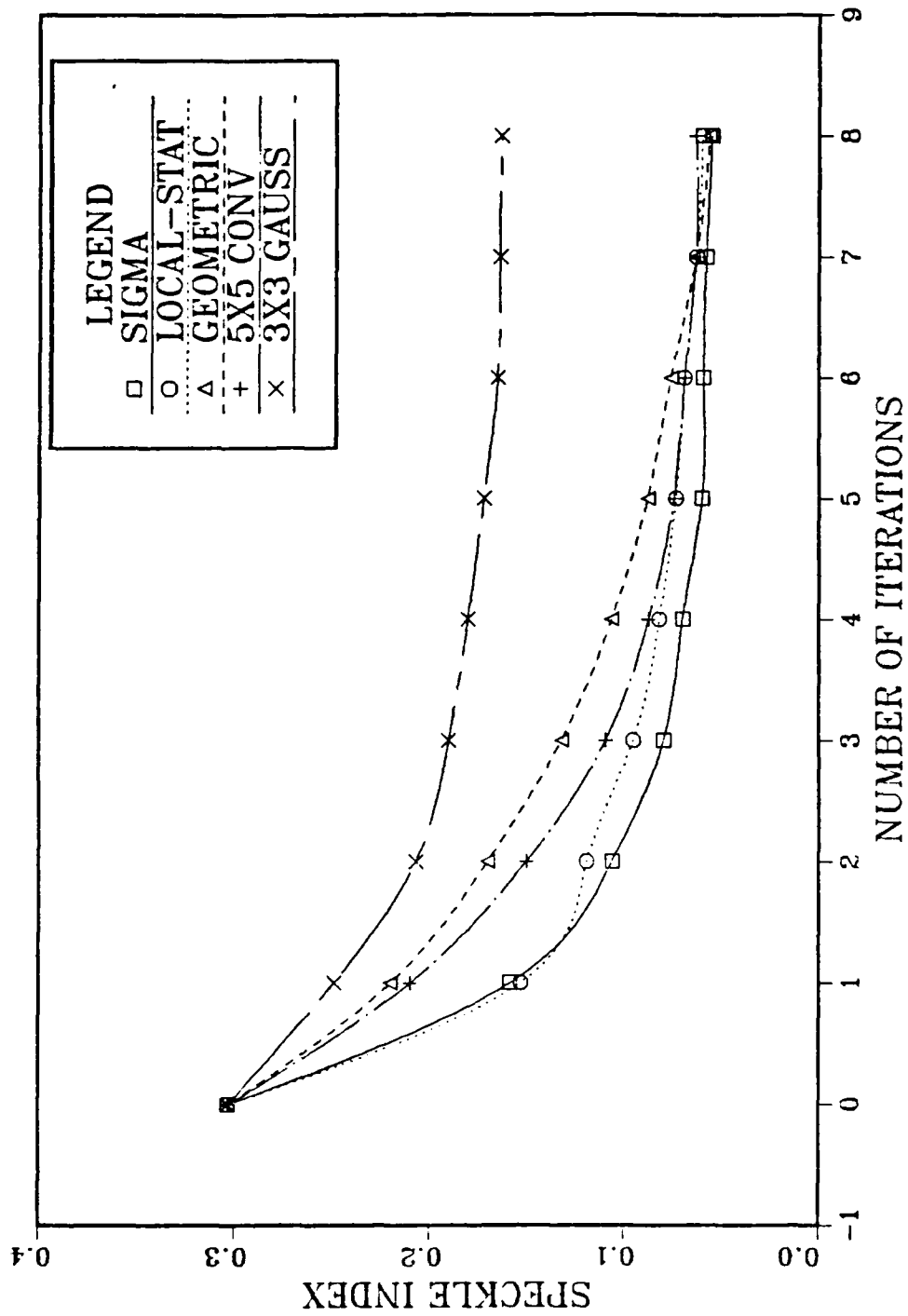


Figure 3.9 Speckle Index Comparison of the Filters.

was very slow and had the least ability to suppress the speckle. After the fourth iteration, its speckle suppression effect is almost lost. At the end of the four iterations, the speckle index was suppressed to 30% of its initial value.

On the other hand, although the Convolution filter can be compared with the nonlinear filters, it is still more gradual at the first 6 iterations. For more iterations, it will have almost the same effect with the others. The 5x5 Convolution filter reaches a 60% speckle index suppression after the fourth iteration.

2. Comparison of the Times Needed per Iteration

As discussed before, the Gaussian and Convolution filters are considerably faster than the nonlinear filters. This is the major advantage of these filters. The times needed for one iteration of each filter are given in Table 1.

TABLE 1
TIMES PER FILTER ITERATION.

Filter	Time
3x3 Gaussian filter	18 sec
5x5 Convolution filter	38 sec
Sigma filter	2 min, 15 sec
Geometric filter	5 min, 44 sec
Local Statistics filter	13 min, 45 sec

When the times needed per iteration for the nonlinear filters were compared with the values previously measured [Ref. 3: p. 34], it was found that the speeds had improved. This is due to the installation of an upgraded processor board with a 386 microprocessor. The times for the nonlinear filters are still considerable, because these filters need to be run for more than one iteration.

3. Visual Comparison and Resolution Degradation

Another criterion used to evaluate the performance of any filter is to test its resolution preserving ratio. All filters tend to smear and blur the edges of the image while suppressing the speckle. Measuring the distortion visually is a subjective process and changes slightly for each person. To avoid the subjective judgement, the AFRT was used to resolve the resolution degradation of the each filter.

Figure 3.10 shows a comparison of the measured resolution for each of the filter types. The horizontal axis shows the number of iterations of the filter. Each iteration reduces the speckle further. Resolution of the original image after thresholding was 12.4 microns. At the first iteration, all filters have almost the same resolution degradation. As can be seen clearly in Figure 3.10, the Gaussian filter has the least resolution degradation, but on the contrary its speckle reduction capability is the worst. On the other hand, the 5x5 Convolution filter, while fast, has the most resolution degradation. This is the major disadvantage of the 5x5 Convolution filter. Although this filter might be compared with the other nonlinear filters like the Geometric, the Sigma and the Local Statistics filters to beat down the speckle, its resolution capability is the worst at retaining the edges, basic shape and size of the objects. This can also be seen by close comparison of Figures 3.8a and 3.8b.

As a conclusion, the locally developed filters will not bring any major advances in combining speckle reduction, operating speed, and resolution degradation. The Geometric filter can still be accepted as the best overall filter from the points of view suppressing the speckle and retaining the basic shape and size of the objects [Ref. 3: p. 39] at the expense of requiring almost six minutes per iteration.

COMPARISON OF THE FILTERS

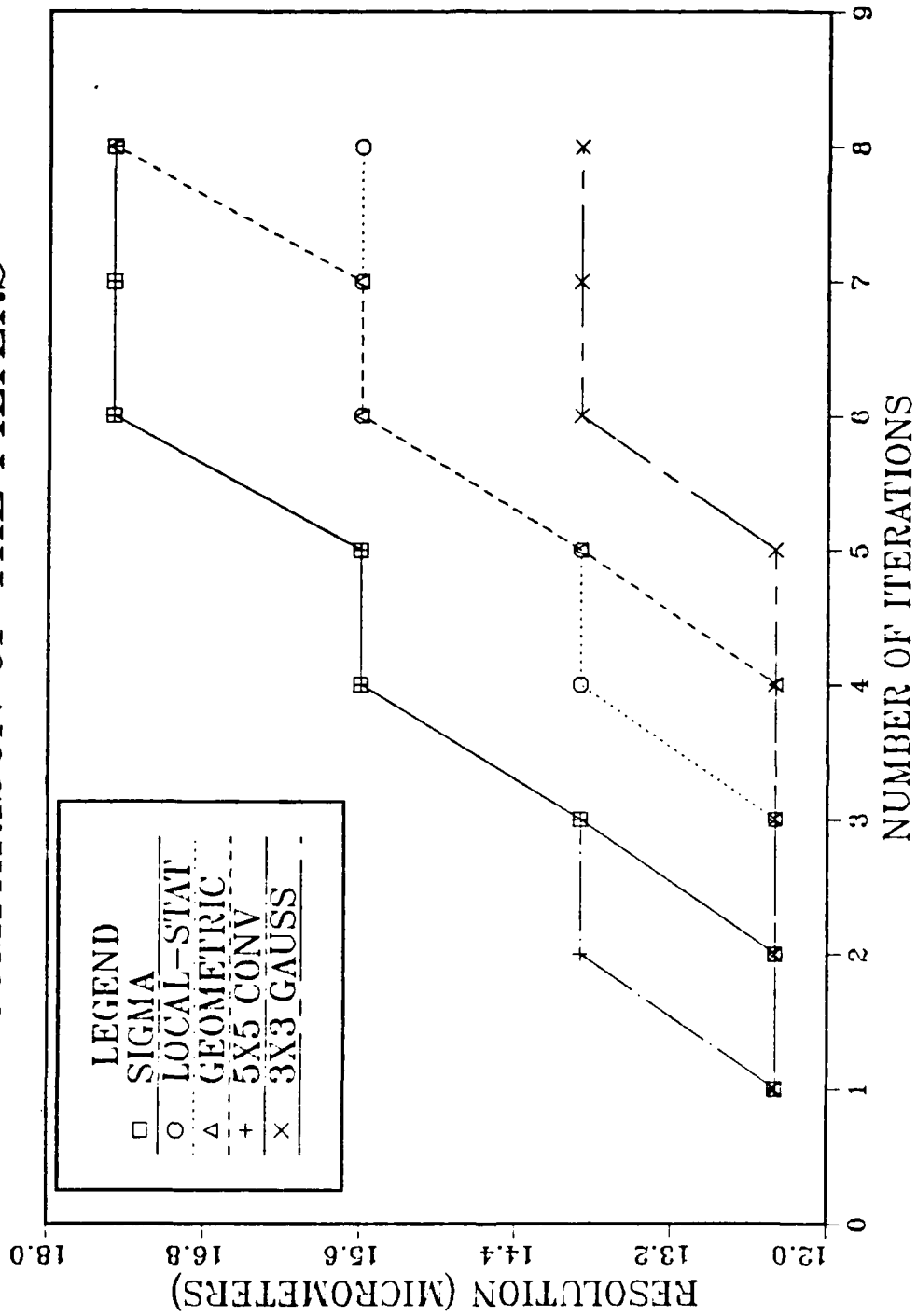


Figure 3.10 Comparison of the Resolution Degradation.

IV. PARTICLE DATA ACQUISITION AND MEASUREMENT RESULTS

The acquisition and digitization of the image along with preliminary processing and sizing techniques have been summarized in the previous chapters. It is important to recall that the main goal of this investigation was to produce a system that is capable of measuring the quantity and size of the particles in the combustion chamber of a rocket motor. The particles are expected to be nearly spherical in shape and range in size from 1 micron to 200 microns in diameter.

A. THE PROCESS BREAKDOWN

Once the hologram has been successfully recorded, a computer process measures the particle size and produces a statistical description of the particle size distribution. The steps required to produce this distribution can be summarized as follows:

1. Image acquisition from the hologram reconstruction. During the reconstruction phase, the real image of one field of the reconstructed hologram is focused on a spinning mylar disk. The disk motion temporally varies the speckle pattern, while the particle images remain stationary during the 1/30 of a second integration time of the vidicon. Then the real image of the selected field is recorded by the VCR through a microscope. The same process is repeated to scan the entire hologram reconstruction volume. Each view should produce an independent set of particles.
2. Image digitization and storage on the computer system. The ImageAction or the Itex PC software functions are used in conjunction with the PC Vision plug-in board for this purpose.
3. Speckle reduction filtering to separate the particle image information from the overlaying speckle. An investigation into the tradeoff between resolution, speckle reduction, and the time needed for one iteration of the filter was discussed in the previous chapter.
4. Application of an image threshold to separate the image features from the background features. Direct observation is the usual method to evaluate the effectiveness of the threshold value. Histograms of the original image and the filtered image are good indicators to aid the user in making a decision about the location of the threshold.
5. Feature identification to find the connected feature pixels and to recognize the connected pixels as a single object. As previously described, a Fortran program processes the thresholded image for object identification and counting. The object identification is done by scanning the image for adjacent pixels (at the horizontal, vertical and right-upper diagonals only). Adjacent pixels are joined to form one *object* or *feature*.

6. Feature sizing to produce the data table. The area and the maximum chord widths are then computed for each feature and written into a data table. (If desired, a roundness test can be applied to the chord length measurements to eliminate nonspherical particles).
7. Producing the histogram of the data table. The data table is transferred into the STATGRAPHICS software, and the histogram is produced by using the STATGRAPHICS functions.
8. To obtain the total particle distribution of one hologram, all steps are repeated for the different fields of the hologram depending on the magnification. Then, the local histograms are added to each other using the STATGRAPHICS functions.

B. CURRENT MEASUREMENT RESULTS

During the reconstruction phase, the field of view of the microscope system is determined by the magnification required to resolve the smallest particle. Also, the number of particles within the field of view depends on the magnification of the microscope system. One question of interest, then, was how many particles were enough to provide a meaningful set of statistics. Figure 4.1 shows a frequency histogram of particle size distribution as measured from a calibration array hologram. The horizontal axis is the x-width of the particle. This histogram shows the particle distribution of 96 particles. Figure 4.2, 4.3 and 4.4 show the data from a various number of fields of view from the same hologram image. These histograms are the distributions of 681, 984 and 1592 particles from 7, 10 and 16 fields of view, respectively. As can be seen from the figures, Figure 4.3 has the general shape of the distribution from larger numbers of particles for this hologram. As an initial observation, we have experimentally concluded that approximately 1,000 particles need to be measured before the distribution stays about the same (for the hologram used). This observation was verified by using an experimental hologram taken during a rocket firing. The five different fields of view of this hologram which also include about 1,000 particles, verified the expected shape of the distribution. Figure 4.5 represents the data from 288 particles in one field of view. Figure 4.6 represents the data from 909 particles in three fields of view. Figure 4.7 represents the data from 1179 particles in five fields of view.

So, it can be generalized that the histogram of particle size distribution reaches a representative shape after summing information from approximately 1,000 particles. Further experimentation is necessary to establish confidence levels in the data for different types of images.

Frequency Histogram of X_Chord
 (96 Particles)

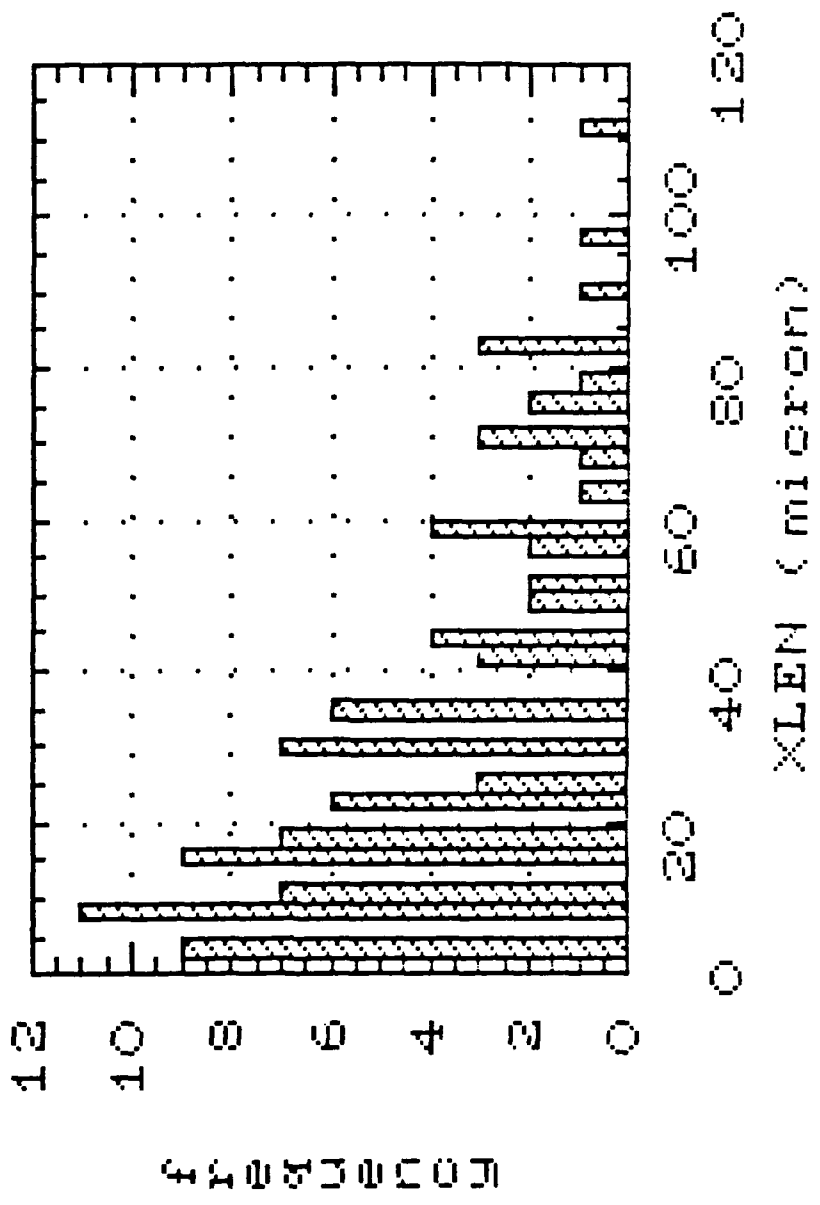


Figure 4.1 Particle Distribution of One Field of View
 in the Calibration Array.

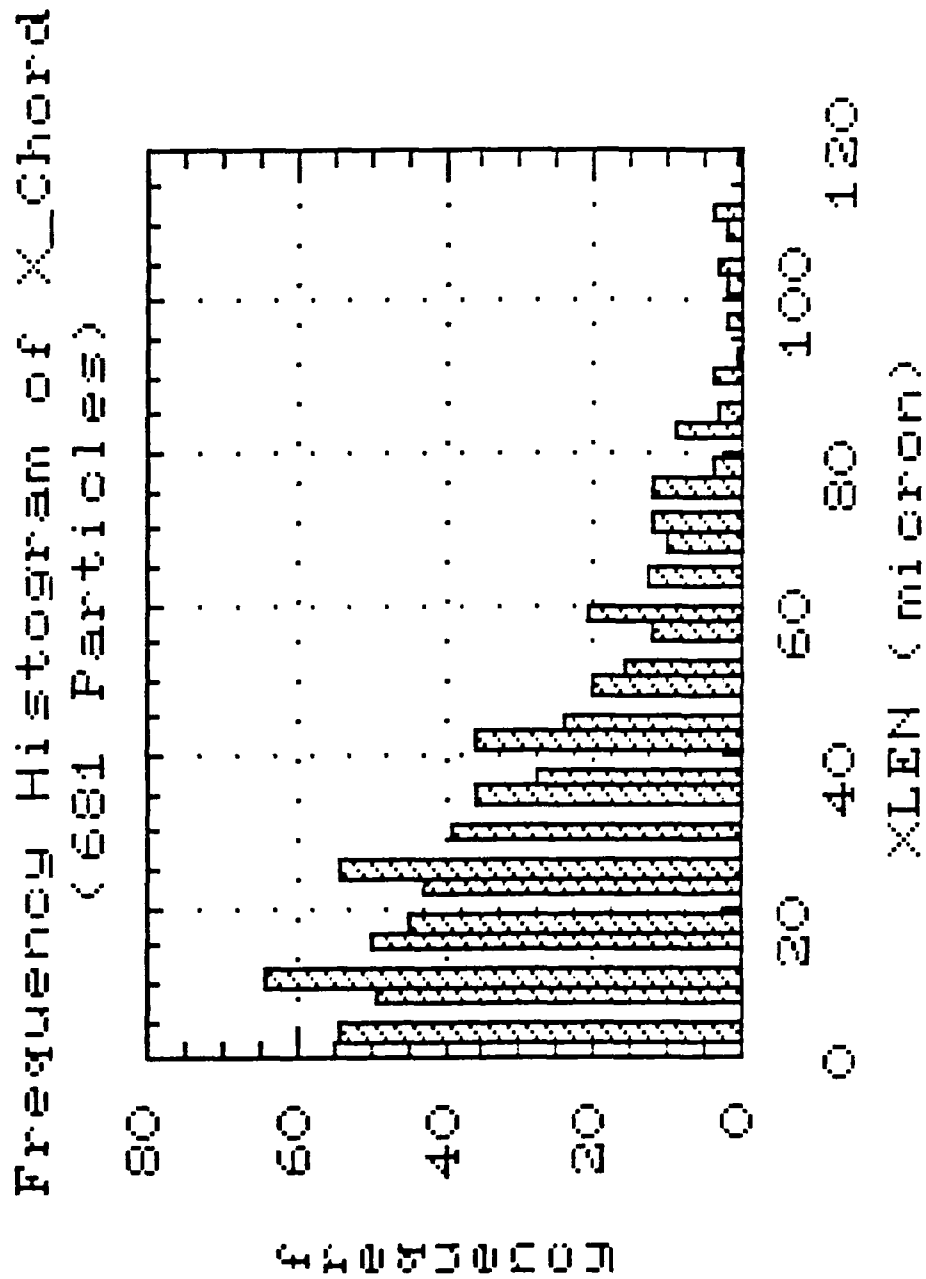


Figure 4.2 Particle Distribution of Seven Fields of View in the Calibration Array.

Frequency Histogram of X_Chord
 (984 Particles)

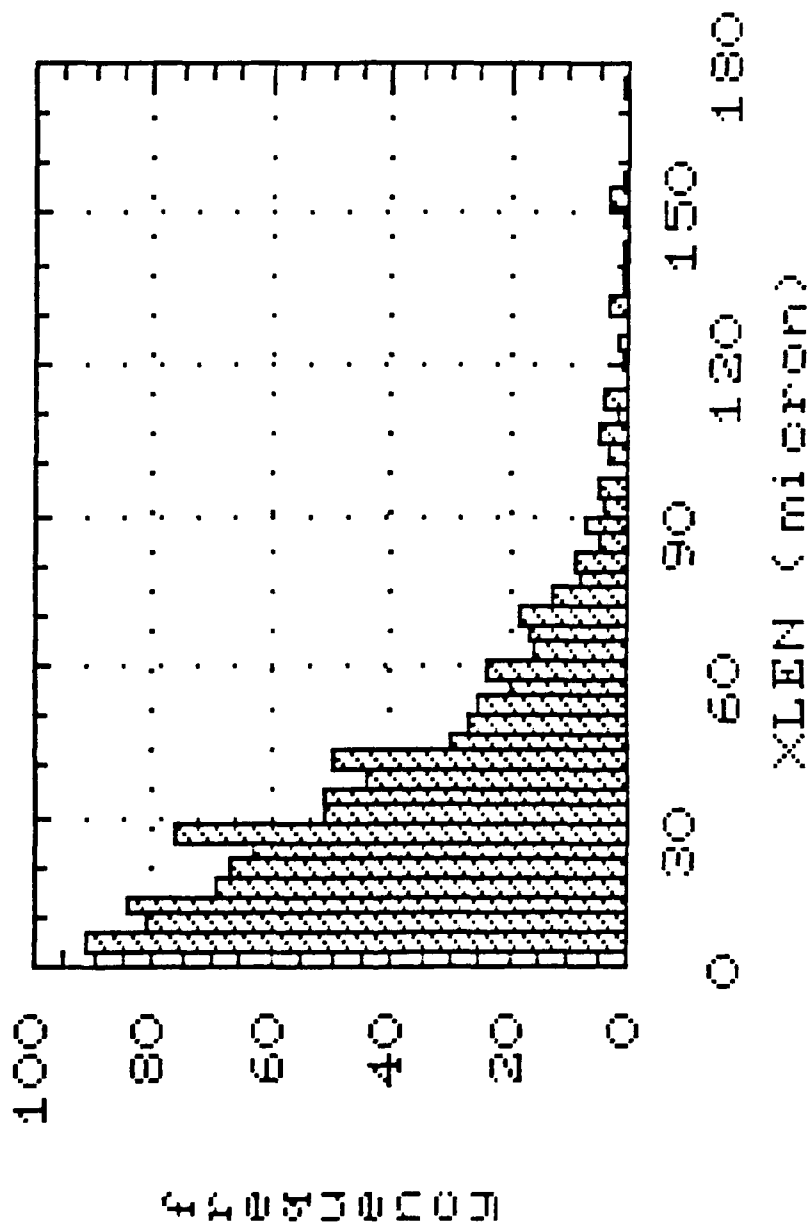


Figure 4.3 Particle Distribution of Ten Fields of View
 in the Calibration Array.

Frequency Histogram of X_Chord
 (1592 Particles)

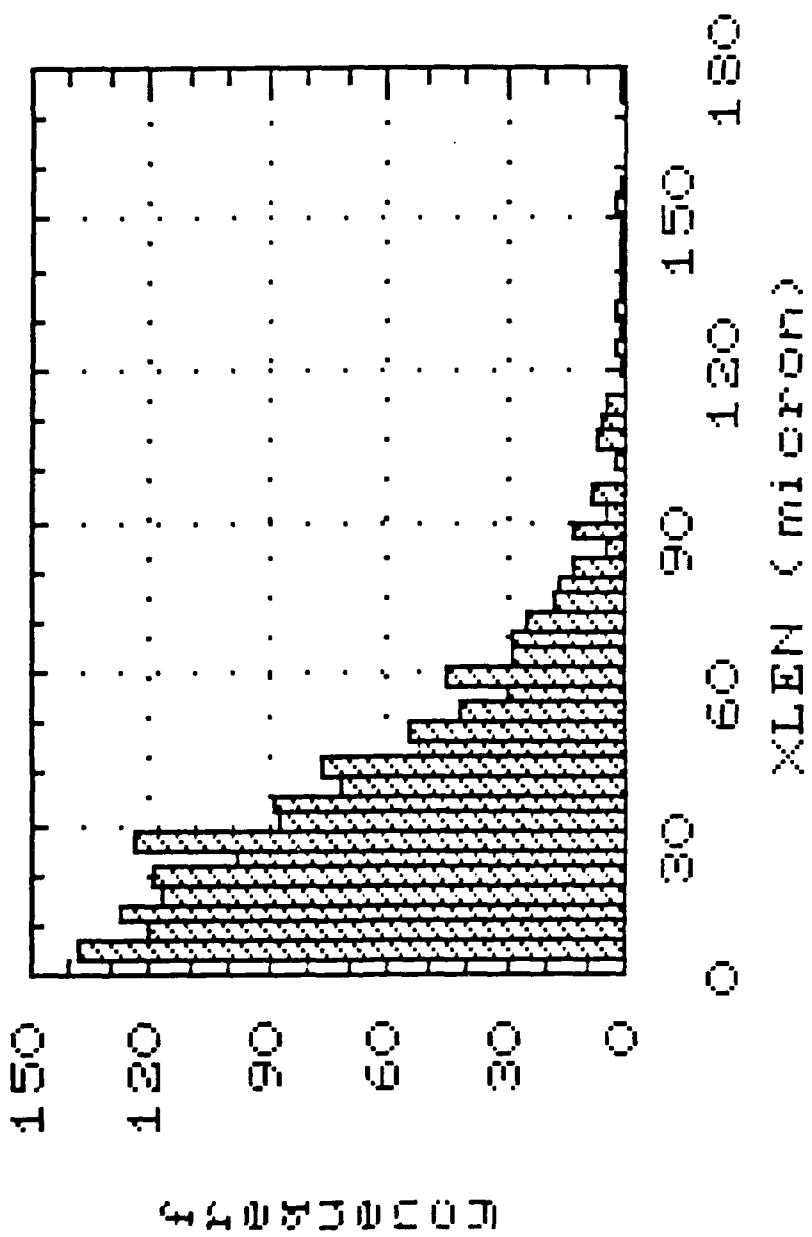


Figure 4.4 Particle Distribution of Sixteen Fields of View in the Calibration Array.

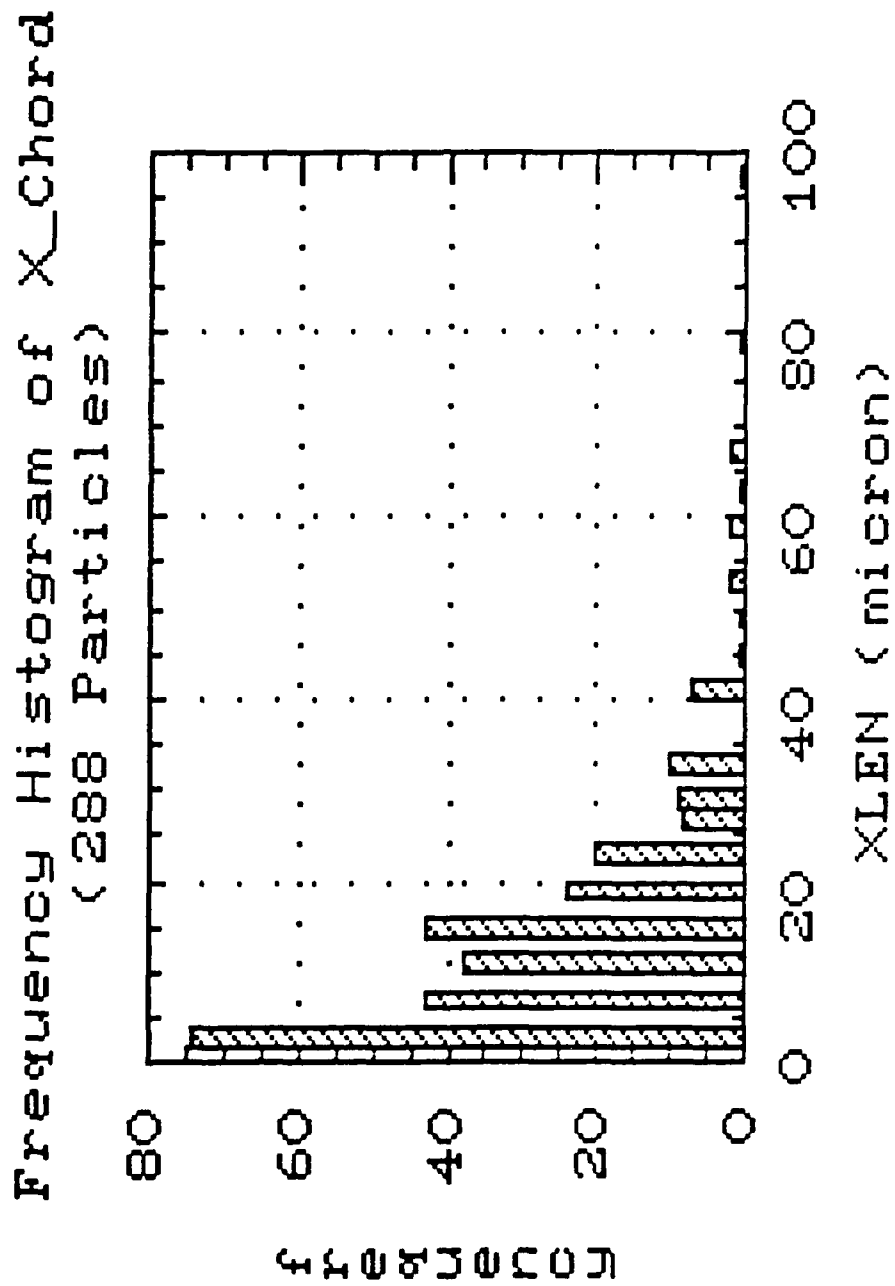


Figure 4.5 Particle Distribution of One Field of View in the Real Combustion Hologram.

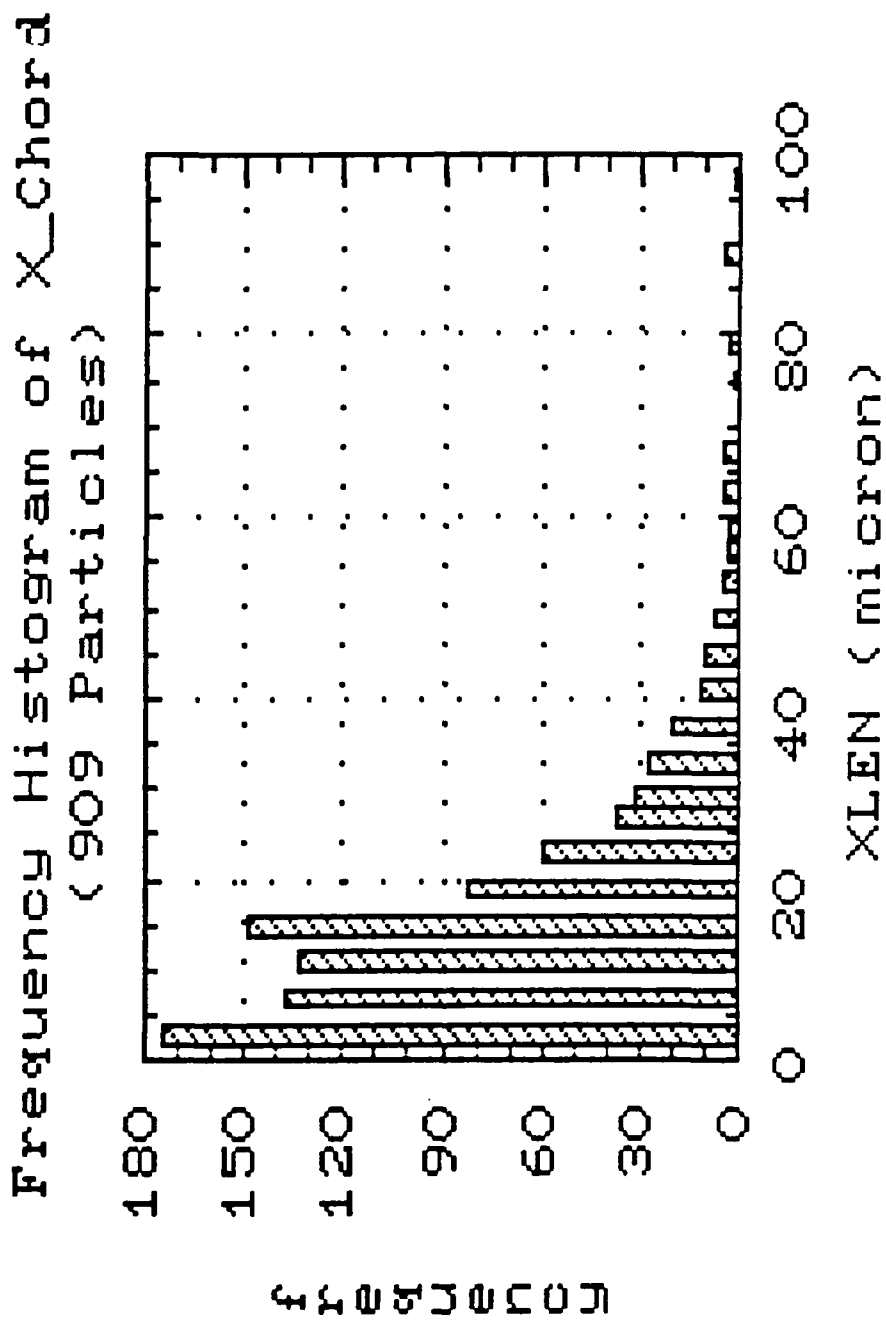


Figure 4.6 Particle Distribution of Three Fields of View in the Real Combustion Hologram.

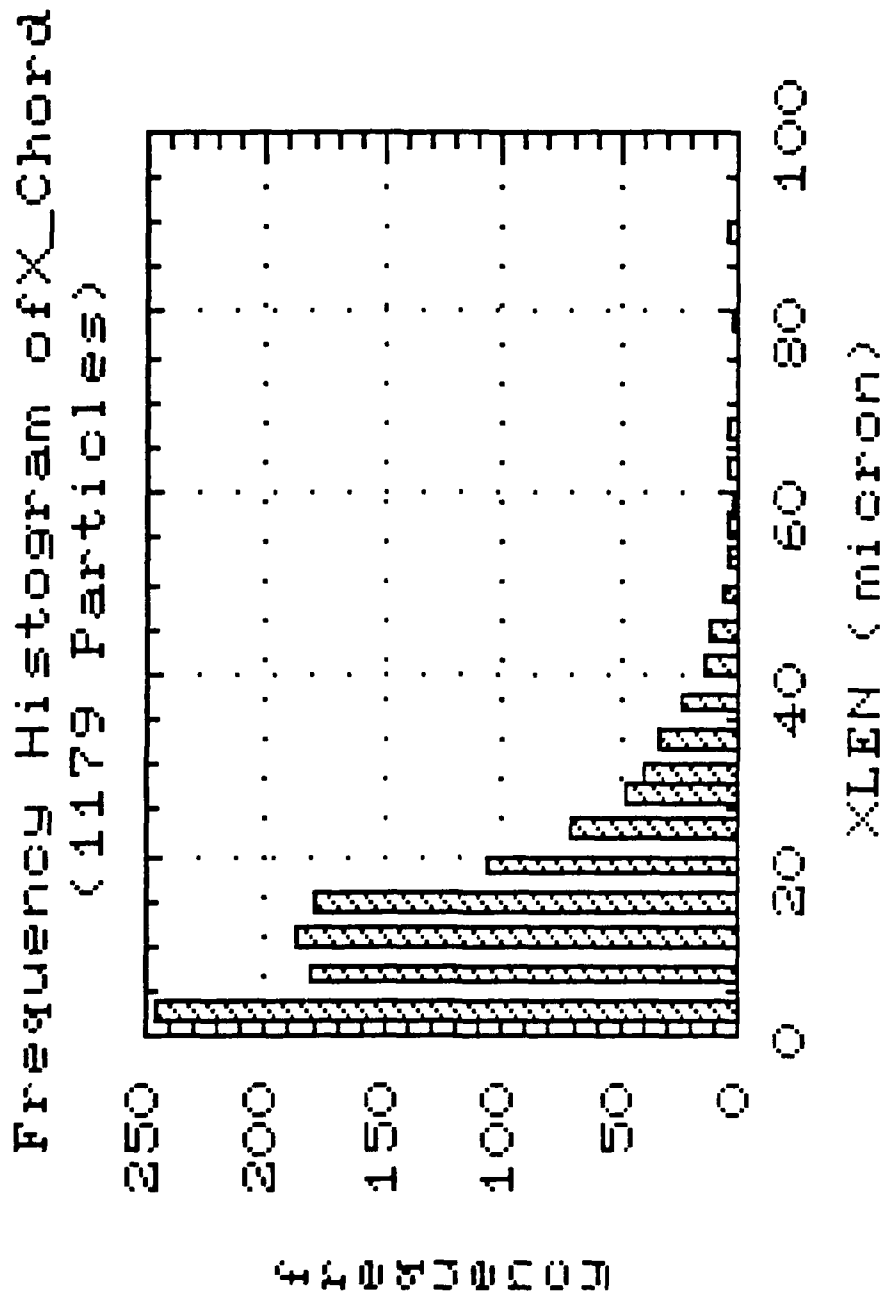


Figure 4.7 Particle Distribution of Five Fields of View in the Real Combustion Hologram.

C. CONSTRAINTS OF THE PROCESS

The major remaining problem for this investigation is the time to process the images. Although improvements were provided, it still takes significant time to run the programs. The solutions for reducing the time-delay can be classified into two categories: hardware and software improvements.

1. *Hardware Solutions:*

1. The IBM/AT microcomputer is the heart of the system, and it uses the IBM-DOS (Disk Operating System) Version 3.1. DOS has some limitations handling more than 20 buffers. Therefore, it is difficult to load the entire screen image into a two-dimensional array. However, in the future, using the primary memory in order to process the image will speed up the entire process.
2. The IBM/AT microcomputer already has an upgraded processor board with a 386 microprocessor, which runs at 16 MHz. The system speed can be increased by using the more powerful and faster computers.

2. *Software Solutions:*

1. Current locally developed programs have been written in Fortran. Using another computer languages like Pascal, C or Assembler can be expected to be more effective in speeding up the process.
2. The developed Fortran routines have an interactive structure. At first, the user has to describe the local window dimensions before the program runs. (The details about the window are in Chapter Two.) This is an obstacle for automatic operation, since the program depends on the user's observations to describe the dimensions of the window. Description of an optimal and fixed-dimension window would help the automation of the process.
3. The feature identification routine has already been written to test the adjacent pixels in order to describe a feature in the horizontal, vertical and right-upper diagonal directions. The algorithm can be improved by checking the other diagonals. This might decrease the time needed to join adjacent pixels into identified features.

V. CONCLUSIONS

The results of this investigation show that the IBM/AT microcomputer with a dedicated software, fast-access image memory board, and 16 MHz. 386-microprocessor is a viable system to process the hologram images. Now, 512 x 512 images can be handled in 10 minutes from frame digitization to production of the data table. Higher processing rates can be achieved with faster computers. The time currently required is appropriate for the feasibility studies which were carried out.

As an initial observation, the data from independent views of the reconstruction studied suggests that the histogram of the particle size distribution reaches a representative shape after summing information from approximately 1,000 particles. Further study is needed to verify this initial observation.

As a result of image enhancement and filtering investigations, the Geometric filter has been found to be the best compromise filter among the others. Because locally developed filters (like 3x3 Gaussian filter and 5x5 Convolution filter) do not have any analytical representation for the speckle, they are not as successful as the nonlinear filters (the Geometric filter, the Sigma filter, and the Local Statistics filter). Especially, the 5x5 Convolution filter has the worst resolution degradation property. Much more improvement can be made toward reducing the speckle degradation due to filtering.

There is still a need to improve the hologram recording and reconstruction techniques. Currently, resolution of the original images is about 12 microns. Better optics will also help in achieving better reconstruction.

The locally developed routines have been written in Fortran. Using computer languages like Pascal, C, and Assembler might be helpful to improve the speed of the computer processing.

The Feature Identification routine tests the pixels to identify the features at the horizontal, vertical, and right-upper diagonal directions. Checking the other diagonals to identify the features might reduce the processing time.

The Feature Identification and Sizing Fortran routines need a description of a local window which will be able to cover the largest feature in the current screen. This is the weak point of the programs in the view of automation of the process. Later

studies need to investigate whether a fixed size window can solve this problem, and whether different fields of the hologram can be processed with an automatic process.

The 4x magnification of the microscope proved to provide a reasonable processing time for one feature in one field of image and a resolution increment of 3.7 microns. As the magnification of the microscope increases, the resolution increment becomes smaller, more sensitive, and the resolution degradation decreases. This concurrently increases the processing time. However many more fields of view are required to cover the hologram reconstruction volume. Further investigation is needed to study the tradeoffs required.

APPENDIX
LIST OF ABBREVIATIONS

STATGRAPHICS	Statistical Graphics System
VCR	Video Cassette Recorder
AOI	Area of Interest
VMB	Video Memory Board
SAR	Synthetic Aperture Radar
AFRT	Air Force Resolution Target
SI	Speckle Index
USAF	United States Air Force
IBM	International Business Machines
DOS	Disk Operating System

LIST OF REFERENCES

1. Orguc, E. S., Pruitt, T. E., Edwards, T. D., Youngborg, E. D., Powers, J. P., and Netzer, D. W., *Measurement of Particle Size in Solid Propellant Rocket Motors*, to be published in Proceedings of the 24th JANNAF Combustion Meeting, Naval Postgraduate School, Monterey, CA, October 1987.
2. Redman, D. N., *Image Analysis of Solid Propellant Combustion Holograms Using an ImageAction Software Package*, Master's Thesis, Naval Postgraduate School, Monterey, CA, June 1986
3. Edwards, T. D., *Implementation of Three Speckle Reduction Filters for Solid Propellant Combustion Holograms*, Master's Thesis, Naval Postgraduate School, Monterey, CA, December 1986.
4. Netzer, D. W., and Powers, J. P., *Particle sizing in Rocket Motor Studies Utilizing Hologram Image Processing*, Proceedings of the NASA Workshop on Data Reduction from Images and Interferograms, NASA Ames Research Center, January 1985.
5. Edwards, T. D., Horton, K. G., Redman, D. N., Rosa, J. S., Rubin, J. B., Yoon, S. C., Powers, J. P., and Netzer, D. W., *Measurements of Particles in Solid Propellant Rocket Motors*, Proceedings of the 21th JANNAF Combustion Meeting, Chemical Propulsion Information Agency, John Hopkins University, Laurel, Maryland, pp. 119-132, 1986.
6. Imaging Technology Incorporated, *The ImageAction User's Guide*, Publication 47-S00003-02, Version 2.0, May 1985
7. Imaging Technology Incorporated, *The Itex'PC Programmer's Manual*, Part Number 47-S00003-02, Version 1.1, September 1985
8. Crimmins, T. R., *Geometric Filter for Speckle Reduction*, Optical Engineering, Vol. 5, No. 5, pp. 651-654, May 1986.
9. Crimmins, T. R., *Geometric Filter for Speckle Reduction*, Applied Optics, Vol. 24, No. 10, p. 1438 May 1985.
10. Lee, J. S., *Speckle Suppression and Analysis for Synthetic Aperture Radar*, Optical Engineering, Vol. 25, No. 5, pp. 636-643, May 1986.

11. Statistical Graphics Corporation, *Statistical Graphics System*, (STATGRAPHICS), STSC, 1986.
12. Gonzales, R. C. and Wintz, P., *Digital Image Processing*, Addison-Wesley Publishing Company, 1977.

INITIAL DISTRIBUTION LIST

	No. Copies
1. Defense Technical Information Center Cameron Station Alexandria, VA 22304-6145	2
2. Library, Code 0142 Naval Postgraduate School Monterey, CA 93943-5002	2
3. Department Chairman, Code 62 Department of Electrical and Computer Engineering Naval Postgraduate School Monterey, CA 93943-5000	1
4. Professor J. P. Powers, Code 62Po Department of Electrical and Computer Engineering Naval Postgraduate School Monterey, CA 93943-5000	3
5. Professor D. W. Netzer, Code 67Nt Department of Aeronautics Naval Postgraduate School Monterey, CA 93943-5000	2
6. Air Force Astronautics Lab Attention : Lieutenant M. Moser Edwards Air Force Base, CA 93523	1
7. Deniz Kuvvetleri Komutanligi Personel ve Egitim Daire Bsk.ligi Bakanliklar , Ankara / TURKEY	3
8. Emin Sami Orguc 1783 Sk. Ali Cebeci Apt. No: 53 / 1 Osmanzade- Karsiyaka Izmir / TURKEY	4